

Hardware-in-the-loop Simulation Method for a Wind Farm Controller Using Real Time Digital Simulator

Gyeong-Hun Kim[†], Jong-Yul Kim^{*}, Jin-Hong Jeon^{*}, Seul-Ki Kim^{*}, Eung-Sang Kim^{*},
Ju-Han Lee^{**}, Minwon Park^{**} and In-Keun Yu^{**}

Abstract – A hardware-in-the-loop simulation (HILS) method for a wind farm controller using a real time digital simulator (RTDS) is presented, and performance of the wind farm controller is analyzed. A 100 MW wind farm which includes 5 MW wind power generation systems (WPGS) is modeled and analyzed in RSCAD/RTDS. The wind farm controller is implemented by using a computer, which is connected to the RTDS through transmission control protocol/internet protocol (TCP/IP). The HILS results show the active power and power factor of the wind farm, which are controlled by the wind farm controller. The proposed HILS method in this paper can be effectively utilized to validate and test a wind farm controller under the environment in practice without a real wind farm.

Keywords: Hardware in the loop simulation, Real time digital simulator, Wind farm controller

1. Introduction

Among the renewable energy such as wind turbines, photovoltaic, fuel cells, micro gas turbines, and, small hydro units, wind turbines have significantly increasing all over the world [1]. According to global wind energy council, a total of 282 GW is now installed in 2012, and an increase in installed cumulative capacity of a wind power generation system (WPGS) is about 18.6% compared to the previous year [2].

Increase of wind farm in power system affects the power balancing between generated and demanded power caused by unstable wind velocity [3]. Unstable wind velocity can cause significant variation in the system frequency that may affect grid system stability [4]. Hence, the grid system operators in many countries such as Denmark, Germany, Spain, US, China, and so on requires grid code for a WPGS or a wind farm [5, 6].

For satisfying the grid code, a wind farm controller (WFC) is needed because it requires the possibility for controlling active and reactive power in point of common coupling (PCC), continuous operation in a limited range, and rate limit operation. The WFC should have ability to sending out set points to all WPGSs, and each WPGS must be able to ensure set points from the WFC. It enables the wind farm to control active and reactive power in PCC [7].

Before the WFC is applied to the wind farm, it is difficult to evaluate and validate the WFC because of security

problem of the power system, cost, and development time. This paper presents performance analysis method without a wind farm to evaluate a WFC using hardware-in-the-loop-simulation (HILS) using a real time digital simulator (RTDS).

A 100 MW wind farm which is composed of twenty 5 MW WPGSs is modeled in RSCAD / RTDS for applying the proposed performance analysis method using HILS, and the modeled wind farm is simulated at real time by the RTDS. The control algorithm [8] of WFC is implemented using C# programming language in a computer. A communication interface between real time simulation and the WFC is also implemented through TCP/IP.

The HILS results show the active power and power factor at PCC of the wind farm controlled by the WFC. The dynamic performances of several wind turbines are also depicted when they are controlled by the WFC. Using the proposed HILS method, a newly designed and developed WFC can be effectively tested and validated under the environment in practice without a real wind farm.

2. Wind farm model

The configuration of a wind farm is depicted in Fig. 1, which is modeled in RTDS. A total rated power of the wind farm is 100 MW, and it has twenty WPGSs, a substation.

It is made up of 5 MW variable speed WPGS, which use a permanent magnet synchronous generator (PMSG) and a back-to-back voltage source converter. The WPGS is connected to medium-voltage (MV) at 33 kV. The MV is boosted up to 154 kV by using two 60 MW step-up transformers. The substation is connected to the PCC through 20 km long cable. Table 1 shows parameters of the 100 MW modeled wind farm.

[†] Corresponding Author: Smart Distribution Research Center, Korea Electrotechnology Research Institute, Korea. (kgh1001@keri.re.kr)

^{*} Smart Distribution Research Center, Korea Electrotechnology Research Institute, Korea. (jykim@keri.re.kr)

^{**} Dept. of Electrical Engineering, Changwon National University, Korea. (paku@changwon.ac.kr)

Received: September 5, 2013 ; Accepted: April 16, 2014

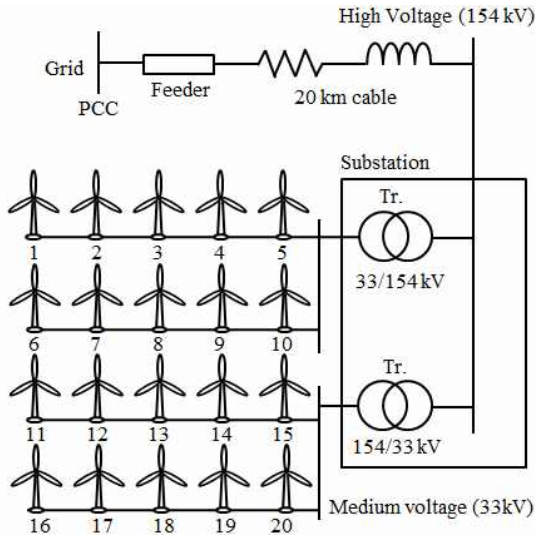


Fig. 1. Configuration of the wind farm

Table 1. Parameters of 100 MW modeled wind farm

Type	Parameters	Values
Wind farm	Total rated power	100 MW
	Number of wind turbine	20
	Distributed voltage	33 kV
	Transmission voltage	154 kV
Substation	Number of Tr.	2
	Rated power	120 MVA
	Leakage inductance of Tr.	0.05
	Voltage	33/154 kV
Feeder	Cable length	20 km
	Resistance	0.19 Ω /km
	Reactance	0.41 Ω /km

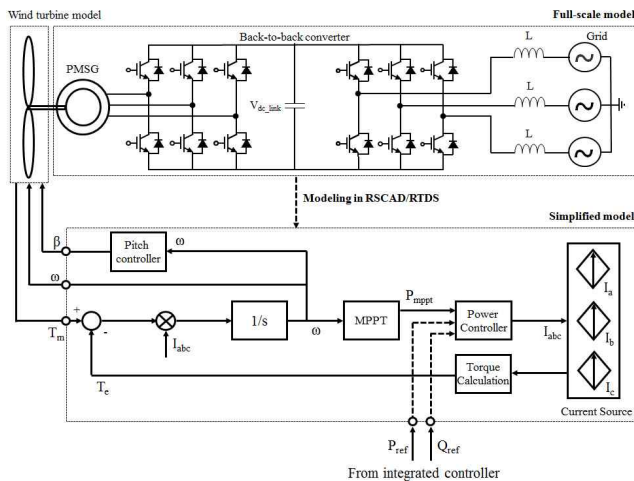


Fig. 2. Configuration of the modeled 5 MW wind power generation system in RSCAD/RTDS

2.1 Modeling of wind power generation system

In this paper, a 5 MW variable speed WPGS is modeled in RSCAD / RTDS. The WPGS consists of the PMSG,

whose stator winding is directly connected to a bidirectional frequency converter made up of two back-to-back IGBT bridge. However, there is a constraint of operation time and processor card [9] of the RTDS for implementing the real time simulation. For the reason, a simplified model of the WPGS [10] is considered as shown in Fig. 2, which includes a three phase current source and wind turbine model.

2.2 Modeling of wind turbine

In the case of the wind turbine model, the mechanical torque (T_m) of the turbine captured from the wind power can be calculated by

$$T_m = \frac{1}{2} \rho \pi R^3 v^2 C_p(\lambda, \beta) / \omega \quad (1)$$

where ρ is the air density (kg/m^3), v is wind velocity (m/s), R is the radius of blade (m), ω is angular velocity (rad/s), C_p is power coefficient [11].

The power coefficient is a function of tip speed ratio (λ) and pitch angle (β) of the blade (degree) as follows (2).

$$C_p(\lambda, \beta) = c_1 \left(\frac{c_2}{\lambda_i} - c_3 \beta - c_4 \right) e^{-\frac{c_5}{\lambda_i}} + c_6 \lambda \quad (2)$$

$$\lambda_i = \frac{1}{\frac{1}{\lambda - 0.08\beta} - \frac{0.035}{\beta^3 + 1}} \quad (3)$$

where c_1 is 0.5176, c_2 is 116, c_3 is 0.4, c_4 is 5, c_5 is 21, and c_6 is 0.0068 [12]. Parameters of the 5 MW wind turbine model are given in Table 2. The maximum power coefficient (C_{p_max}) is 0.48 when tip speed ratio is 8.1 (λ_{opt}).

The controller of maximum power point tracking (MPPT) calculates the power reference (P_{mppt}), which is given by (3).

As in (4), the rotation speed of the wind turbine is used to determine the power reference of MPPT. In the case of over rated power, the power reference is limited to the 5 MW.

$$P_{mppt} = \frac{1}{2} \frac{\rho \pi R^5 C_{p_max}}{\lambda_{opt}^3} \omega^3 \quad (4)$$

Table 2. Parameters of 5 MW wind turbine model

Parameters	Values
Rated wind velocity	11.5 m/s
Radius of the blade length	60 m
Rotation speed	15 rpm
Maximum power coefficient	0.48
Optimal tip speed ratio	8.1
Air density	1.225 kg/m^3
Inertia of the rotor	117,000,000 kgm

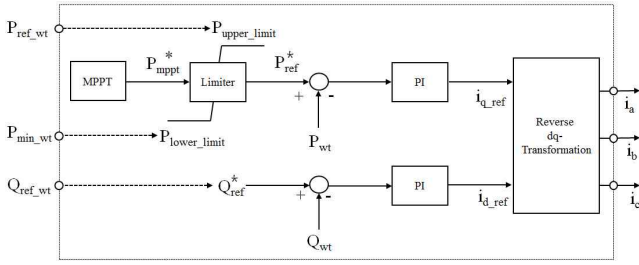


Fig. 3. Power controller of the simplified wind turbine model

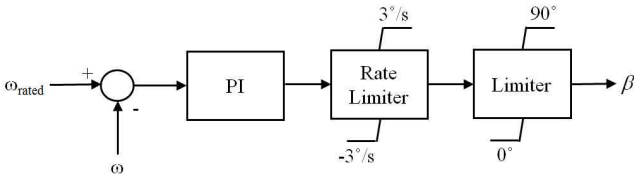


Fig. 4. Block diagram of the pitch angle controller

2.3 Power controller of the simplified model

The three phase current source of the modeled 5 MW WPGS is controlled by power controller as represented in Fig. 3. References of DQ-axis current component frame are used for control of the active and reactive power, whose reference is received from the WFC.

As shown in Fig. 3, the reference power of MPPT control is limited by active power commands (P_{ref_wt} and P_{min_wt}) from the WFC. The reactive power of WPGS is controlled to reactive power commands (Q_{ref_wt}). If the active power command from the WFC is smaller than the reference power of the MPPT control, the output power of wind turbine is limited. It causes an increase of the rotation speed of the wind turbine because of difference in torque between the electrical output power and the mechanical power. In that case, the rotation speed of wind turbine is regulated by pitch angle controller.

Fig. 4 shows the block diagram of the pitch angle controller, which increases pitch angle for the purpose of regulating the rotation speed [13]. The pitch angle is limited to $3^\circ/s$ for realistic response.

3. Implementation of Hardware in the Loop Simulation for Test of Wind Farm Controller

The configuration of HILS setup for test of wind farm controller is depicted in Fig. 5. The WFC is implemented using C# programming language, which is operated by a computer.

The WFC can connect to the real time simulation model of the 100 MW wind farm through an Ethernet switch between RTDS and the integrated controller. It provides the same communication environment in practice. The modeled wind farm is simulated with $50 \mu s$ time step in real time.

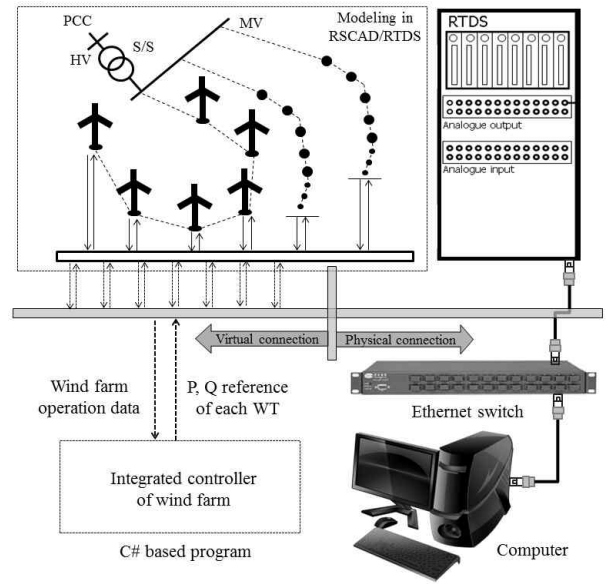


Fig. 5. Configuration of hardware in the loop simulation setup for test of the integrated controller

The operation data such as the total active (P_{wf}) and reactive power (Q_{wf}) of the wind farm, the active and reactive powers of each WPGS (P_{wt}^i and Q_{wt}^i), values of pitch angles and rotation speed is sent to the integrated controller. The integrated controller calculates each WPGS's active and reactive power commands ($P_{wt_ref}^i$ and $Q_{wt_ref}^i$) for controlling the total active and reactive power of the wind farm.

3.1 Wind farm controller

Fig. 6 shows the control algorithm [8] of the WFC. Total active and reactive power references of the wind farm (P_{wf_ref} and Q_{wf_ref}) are required by grid operator. The active power reference of wind farm is limited to 1 MW/s by ramp rate, and the power is controlled by PI controller. The active power reference of each WPGS is calculated by dispatch control and weight value (PF_{wt}^i) in (5).

$$P_{wt_ref}^i = PF_{wt}^i \cdot P_{PI_out}, \quad PF_{wt}^i = \frac{P_{wt_avg}^i}{P_{wf_avg}} \quad (5)$$

The available reactive power of the wind farm depends on the active power because of the current capacity of the back to back converter. The available reactive power of the wind farm is sum of each available reactive power of the WPGSs as follows in (6).

$$Q_{wf_av} = \sum Q_{wt_av}, \quad Q_{wt_av} = \sqrt{P_{rated}^2 - P_{wf_avg}^2} \quad (6)$$

The reactive power reference of each WPGS is also calculated by dispatch control and weight value (QF_{wt}^i) in (5).

4. Hardware in the Loop Simulation Results

Fig. 7 shows the wind speed at number 1, 8, 20 WPGSs used in the real time simulation. The output powers of the wind farm under MPPT operation mode and dispatch operation mode are compared as shown in Fig. 8. All WPGSs operates MPPT control mode during 0 to 175 s. About 175 s, the power reference of the wind farm is 30 MW, which is supposed that the grid operator requires. As shown in Fig. 8, the active power of wind farm is controlled to its reference. At that time, the dynamic performances such as rotating speed and pitch angle of number 1, 8, 20 WPGSs are shown in Figs. 9-11.

The output power of the #1 wind turbine is unchanged after dispatch operation mode as shown in Fig. 9. However, the pitch angle of #1 wind turbine increases under below

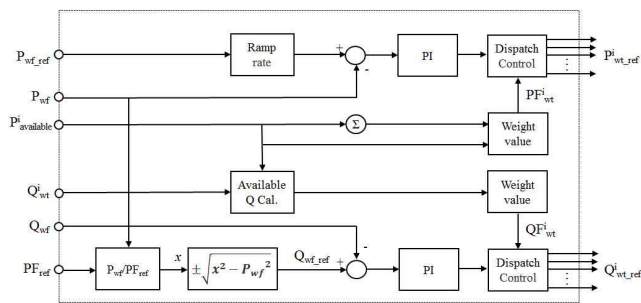


Fig. 6. Control algorithm of the integrated controller

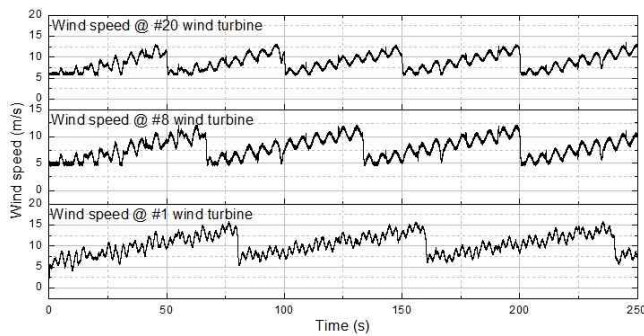


Fig. 7. Wind speed at 1, 8, 20 WPGSs

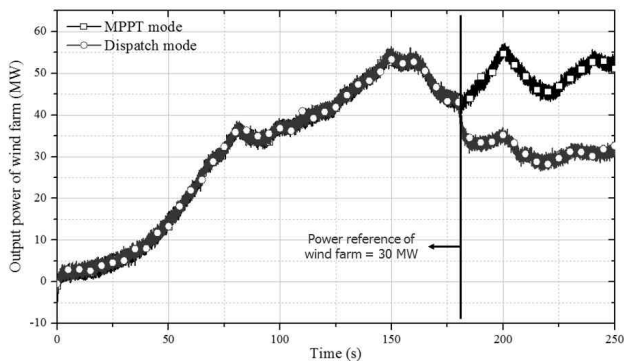


Fig. 8. Output power of the wind farm applying to the integrated controller

rated output power. That means the power reference of #1 wind turbine is limited to about 2 MW from the WFC. In the case of the # 8 wind turbine, the output power is gradually decreases after dispatch operation mode. The rotation speed and pitch angle of # 8 wind turbine are increase because the output power is limited by the WFC. In the case of the # 20 wind turbine, the output power is

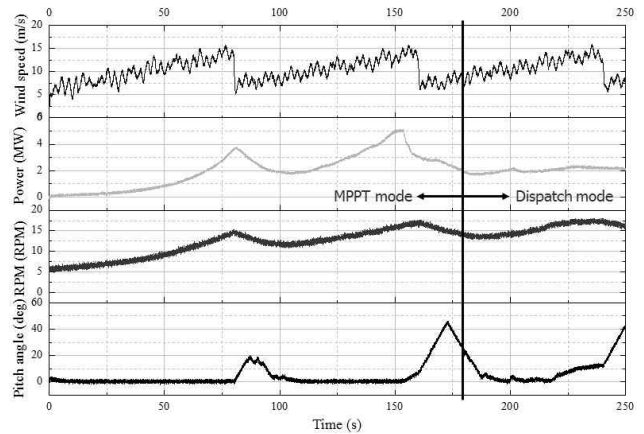


Fig. 9. Wind speed, output power, rotating speed, pitch angle of the #1 WPGS

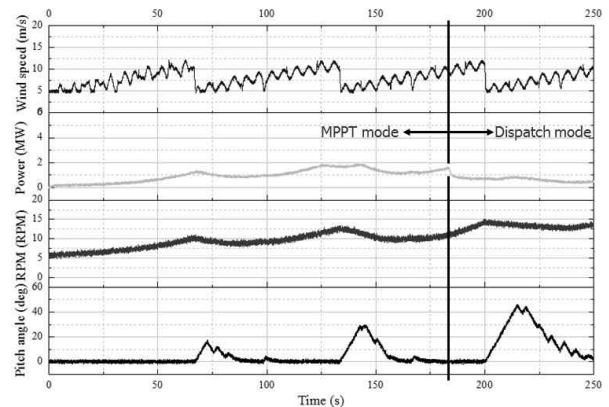


Fig. 10. Wind speed, output power, rotating speed, pitch angle of the #8 WPGS

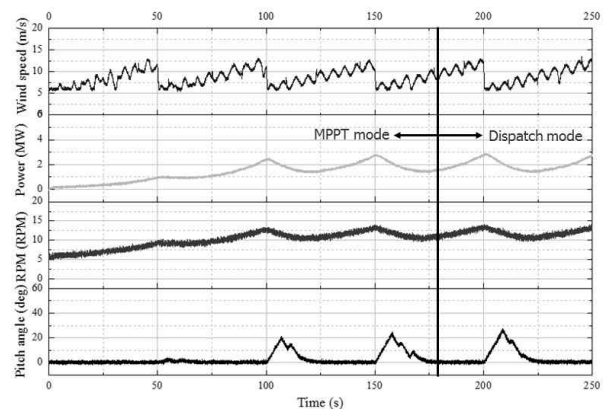


Fig. 11. Wind speed, output power, rotating speed, pitch angle of the #20 WPGS

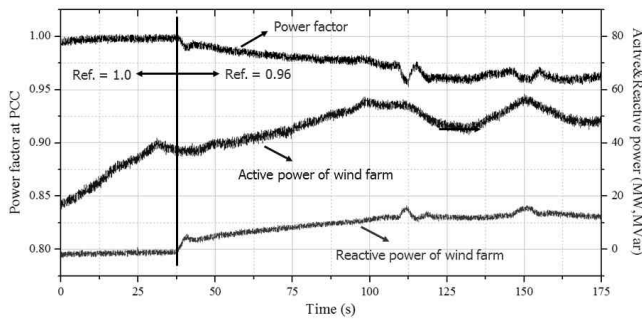


Fig. 12. Power factor and reactive power of wind farm

gradually increases despite of dispatch operation mode. It is expected that the available power of the # 20 wind turbine is high. However, at last, the rotation speed is regulated by pitch angle controller under below rated wind speed. That means the output power of # 20 wind turbine is also limited by the WFC.

The power factor and reactive power of the wind farm is shown in Fig. 12. After 32.5 s, the power factor reference is 0.96, which is supposed that the grid operator requires. After then, reactive power increases follow active power for satisfying power factor reference.

5. Conclusion

Performance analysis method to evaluate the WFC using hardware in the loop simulation (HILS) is presented. The integrated controller with 100 MW wind farm is tested and analyzed by using the proposed method. The test results show that the WFC is well operated under HILS environment. The proposed test method in this paper can be effectively utilized to test and develop a wind farm controller under the environment in practice without real wind farm.

References

[1] Hae-Gwang Jeong, Jong-Hyun Lee, and Kyo-Beum Lee, "A 2nd order harmonic compensation method for wind power system using a PR controller," *Journal of Electrical Engineering & Technology*, Vol. 8, No. 3, pp. 507-515, 2013.

[2] Lauha Fried, "Global wind statics 2012," *Global Wind Energy Council*, Feb. 2013.

[3] Poul Sørensen, Nicolaos Antonio Cutululis, Antonio Vigeras-Rodríguez, Leo E. Jensen, Jesper Hjerrild, Martin Heyman Donovan and Henrik Madsen, "Power Fluctuations From Large Wind Farms," *IEEE Trans. on Power Systems*, Vol. 22, No. 3, pp.958-965, Aug. 2007.

[4] Sung-Eun Lee, Dong-Jun Won, Il-Yop Chung, "Operation scheme for a wind farm to mitigate output

power variation," *Journal of Electrical Engineering & Technology*, Vol. 7, No. 6, pp. 869-875, 2012.

[5] Müfit Altin, Ömer Göksu, Remus Teodorescu, Pedro Rodriguez, Birgitte-Bak Jensen, Lars Helle, "Overview of Recent Grid Codes for Wind Power Integration," *in publication of OPTIM 2010 Conference*, May 2010.

[6] Jun-Bo Sim, Ki-Cheol Kim, Rak-Won Son, Joong-Ki Oh, "Ride-through of PMSG wind power system under the distorted and unbalanced grid voltage dips," *Journal of Electrical Engineering & Technology*, Vol. 7, No. 6, pp. 898-904, 2012.

[7] José Luis Rodríguez-Amenedo, Santiago Arnalte, and Juan Carlos Burgos, "Automatic Generation Control of a wind farm with variable speed wind turbines," *IEEE Trans. on energy conversion*, Vol. 17, No. 2, pp. 279-284, Jun. 2002.

[8] Mufit Altin, Remus Teodorescu, Birgitte Bak-Jensen, Pedro Rodriguez, Florin Iov, Philip C. Kjær, "Wind Power Plant Control – An Overview", *in Proceedings on the 9th International Workshop on Large-Scale Integration of Wind Power into Power Systems*, GmbH, 2010.

[9] P. Forsyth, T. Maguire, and R. Kuffel, "Real time digital simulation for control and protection system testing", *in Proc. 35th Annual IEEE Power Electron. Spec. Conference*, pp. 329-335, Jun. 2004.

[10] Gyeong-Hun Kim, Hyeong-Heak Bae, Sang-Yong Kim, ChulSang Hwang, Hyo-Guen Lee, Namwon Kim, Hyo-Rong Seo, Minwon Park, In-Keun Yu, "Application of a Battery Energy Storage System for Power Quality Improvement of Jeju Power System", *in publication of ICEMS 2010 Conference*, Incheon, Korea, Oct. 2010.

[11] Siegfried Heier, "Grid integration of wind energy conversion systems", *John Wiley & Sons Ltd*, pp. 34-36, 1998.

[12] M. Rosadi, S. M. Muyeen, R. Takahashi, J. Tamura, "Transient stability enhancement of variable speed permanent magnet wind generator using adaptive PI-Fuzzy controller", *in publication of Powertech Conference*, Trondheim, pp. 1-6, Jun. 2011.

[13] M. Rasila, "Torque and speed control of a pitch regulated wind turbine", *Technical reporter No. 1A*, Department of Electric Power Engineering, Chalmers University, Goteborg (Sweden), *IEEE PES SM2001 Conference*, Vancouver, Canada, July 2001.



Gyeong-Hun Kim He received his B.S. and M.S. and Ph.D. degrees in Electrical Engineering from Changwon National University, Korea in 2007, 2009, and 2013, respectively. Currently, he is a senior research engineer with the Smart Distribution Research Center, KERI. His research interests are operation and control of a wind power generation system.



Ju-Han Lee He received B.S degree in electrical engineering from Changwon University. His research interests are wind power generation system and power control scheme.



Jong-Yul Kim He received his B.S. and M.S. and Ph.D. degrees in Electrical Engineering from Pusan National University, Korea in 1997, 1999, and 2010, respectively. Currently, he is a senior research engineer with the Smart Distribution Research Center, KERI.



Minwon Park He received B.S degree in Electrical Engineering from Changwon National University in 1997 and his Master's degree and Ph.D. degrees in Electrical Engineering from Osaka University in 2000 and 2002, respectively.



Jin-Hong Jeon He received his B.S. and M.S. from Sungkyunkwan University in 1995 and 1997, respectively, and his Ph.D. from Pusan National University, Korea, in 2012, in the department of electrical engineering. Currently, he is a principal researcher with the smart distribution research center, KERI.



In-Keun Yu He received B.S degree in Electrical Engineering from Dongguk University in 1981 and his M.S. and Ph.D. degrees in Electrical Engineering from Hanyang University in 1983 and 1986, respectively. His research interests are wavelet transform applications, electric energy storage and control systems, peak load management & energy saving systems, PSCAD/EMTDC and RTDS simulation studies, and renewable energy sources.



Seul-Ki Kim He received the B.S., M.S and Ph.D. degrees in electrical engineering from Korea University, Seoul, Korea, in 1998, 2000 and 2010 respectively. Currently, he works as a senior researcher with the smart distribution research center, Korea Electrotechnology Research Institute (KERI).



Eung-Sang Kim He received the B.S. degree in electrical engineering from Seoul National University of Technology and the M.S. and Ph.D. degree in electric engineering from Soong-Sil University. Currently, he works as a director in the smart distribution research center, Korea Electrotechnology Research Institute(KERI), Changwon, Korea.